Design, Fabrication, and Experimental Evaluation of a Power-Operated Kenaf Decorticating Machine

B. Ibrahim*, S. M. Dauda, A. A. Balami, P. A. Idah
Department of Agricultural and Bioresource Engineering, Federal University of Technology Minna, Niger state, Nigeria.

ABSTRACT: Kenaf (*Hibiscus cannabinus* L.) is a renewable bast-fibre crop with broad industrial potential, but its commercial uptake in Nigeria is constrained by labour-intensive, time-consuming retting and by mechanical decorticators that are often unsafe, immobile, costly, and prone to clogging. Objective: to design, fabricate, and experimentally validate a low-cost, locally manufactured power-operated kenaf decorticating machine that improves throughput, fibre yield, and operator safety. Mechanical design and structural checks (ASME) established decorticating force (2,779.5 N), torque (166.8 Nm), shaft sizing (calculated 27 mm; 35 mm provided), and a peak theoretical power requirement of 7.9 kW; belt-drive and gear analyses informed transmission selection and belt tensioning. Performance testing used a Box–Behnken response surface design with four factors (maturity stage, operating speed, stem diameter, moisture content) across 27 randomized runs with replication. Measured responses included throughput, decorticating efficiency, trapped/waste fibre, and fibre-quality indices (length distribution, retention ratio, cleanliness, tenacity, fineness, damage index). Fibre length was measured by calliper; tenacity followed single-fibre tensile testing; cleanliness was determined gravimetrically. ANOVA and RSM were used for model fitting, diagnostics, and multi-response optimisation. The prototype delivered throughput of 72.9–84.3 $kg\cdot h^{-1}$ and decorticating efficiencies of 86.3–90.2%. The quadratic model showed strong predictive power ($R^2 = 0.94$; adj. $R^2 = 0.91$; pred. $R^2 = 0.89$) with validated residual diagnostics. Fibre quality was robust (mean lengths 1,200–1,470 mm; retention ratio 67.0–72.3%; mean tenacity ≈ 18.7 cN/tex; fineness 3.5 dtex; cleanliness 7.8%; damage index 6.3%). Operating speed and moisture content were the dominant factors affecting performance and quality. The locally fabricated decorticator attains internationally comparable performance while lowering extraction costs and improving safety, making it suitable for pilot deployment by farmer cooperatives and SMEs and supporting sustainable bast-fibre value chains.

***KEYWORDS*:** Decorticating force, Design analysis, Fibre, Machine construction, Prototype

[Received Jan. 25, 2025; Revised Jun. 24, 2026; Accepted Jul. 10, 2026] Print ISSN: 0189-9546 | Online ISSN: 2437-2110

I. INTRODUCTION

Kenaf (*Hibiscus cannabinus L.*) is a fast growing bast fibre crop with wide industrial applications in textiles, composites, biofuels, and sustainable materials (Xu *et al.*, 2020; Austin *et al.*, 2024). Despite its potential, large scale utilization in Nigeria remains limited, with annual production hovering around 1,000 tonnes and declining since its peak in 2010/2011 due to poor commercial adoption and inefficient processing systems (Olanipekun and Togun, 2020). Conventional fibre extraction methods, particularly retting, are labour intensive, time consuming, and often yield inconsistent fibre quality. Chemical retting may weaken fibre integrity, while biological retting produces stronger fibres but is slow and difficult to standardize (Yu and Yu, 2010; Hossain *et al.*, 2022).

Mechanical decortication offers a promising alternative, yet existing kenaf decorticating machines in Nigeria are plagued by several shortcomings. They are often characterized by low throughput, frequent clogging, unsafe exposed moving parts, immobility, and high fabrication costs, making them impractical for smallholder farmers (Austin *et al.*, 2024; Oyegbami and Ajijola, 2019). Fibre extraction alone contributes 16.9–20% of total production costs, further discouraging commercial cultivation (Palanikumar *et al.*, 2023; Onuwe *et al.*, 2018). These limitations highlight a clear research gap: while kenaf is globally recognized as a renewable fibre source, there is no affordable, safe, and efficient decorticating technology tailored to local Nigerian conditions.

The objective of this study is to design, fabricate, and experimentally evaluate a power operated kenaf decorticating machine using locally available materials. The distinct contributions of this work are threefold:

1. Engineering innovation – A novel machine design supported by rigorous mechanical analysis of decorticating force, torque, shaft dimensions, and power requirements, ensuring structural integrity and reliable operation (Dauda *et al.*, 2014; Khurmi and Gupta, 2012).
2. Methodological advancement – Application of a Box–Behnken response surface design to systematically evaluate the effects of maturity stage, operating speed, stem diameter, and moisture content on machine performance (Montgomery, 2020).
3. Practical impact – Establishment of new empirical benchmarks for throughput capacity, decorticating efficiency, and fibre yield, demonstrating that locally fabricated machinery can achieve performance comparable to international standards while reducing costs and improving safety (Makanjuola *et al.*, 2019; Müssig *et al.*, 2024).

*Corresponding author: balaibrahimkt58@gmail.com
doi: http://doi.org/10.63746/njtd.v23i2.4387

By bridging this gap, the study contributes to agricultural engineering and fibre processing knowledge. It provides a validated framework for efficient, safe, and sustainable kenaf fibre extraction, supporting Nigeria's agro industrial development and advancing the global transition toward renewable materials (Vayabari *et al.*, 2023).

II. MATERIALS AND METHODS

The materials to be used in the construction include mild steel plates, mild steel pipes, mild steel C-section, hardened tool steel and gears for transmission.

A. *Physical and Mechanical Properties of the Kenaf*

The kenaf stem plant variety V 36 was measured for length, diameter, and stubble height. A vernier calliper was used to measure the stem diameter, and a tape rule was used to measure the stem length. The oven (SearchTech instruments: DHG-9101-2SA) dry technique was used to determine the stem moisture content for 24 hours at a temperature of 104 °C. All measurements were made in the laboratory at a room temperature of 28 °C, according to Dauda *et al.* (2015). Equation 1 was used to ascertain the moisture content, MC (Ailenokhuoria *et al.*, 2020).

$$MC = \frac{W_1 - W_2}{W_2} \times 100 \qquad (1)$$

Where W_1 and W_2 are the masses of samples before after drying in kg respectively. The highest plant height measured was 312 cm, while the lowest was 150 cm; the largest stem diameter was 29 mm, while the lowest was 15 mm; and the moisture levels ranged from 72% to 75% (wet basis).

Dauda *et al.* (2014) examined the mechanical properties of kenaf of variety V36 at moisture contents of 35%, 55%, and 72%. The study found that the maximum cutting force and shearing energy were 1584.55 N and 8.75 J, respectively, for 35% moisture content, and 694.86 N and 3.50 J for 72% moisture content. As a result, 694.86 N is used as the crushing force for kenaf stem.

B. *Design Analysis*

The objective of the design analysis was to carefully evaluate the factors needed for fabrication of the machine, ensuring reliability, efficiency, durability, safety, and affordability for the end users. Figure 1 presents the the machine geometry and component layout used for fabrication and FEA input.

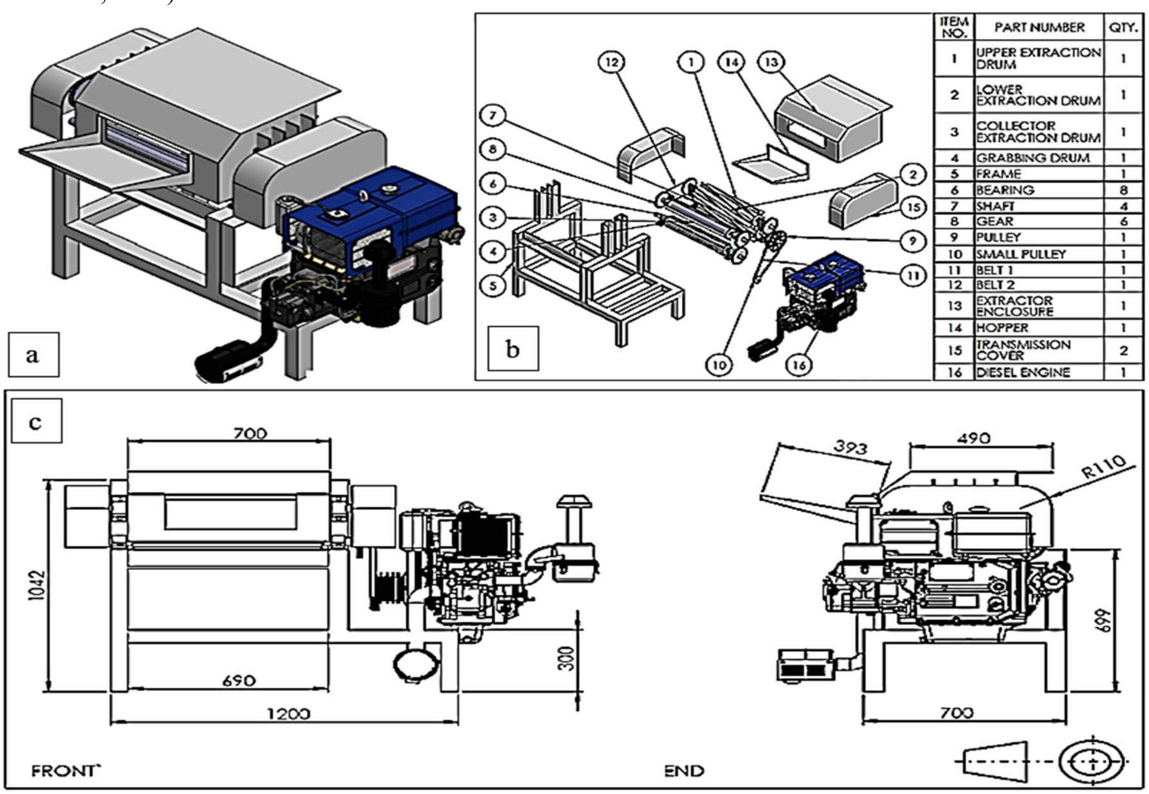

Figure 1 Working drawing of the machine. a. Isometric projection, b. Exploded view, c. Orthographic view

The isometric and exploded views clarify component interfaces (frame, drums, blades, pulleys), while the orthographic projection provides the exact dimensions used in strength and kinematic calculations. These drawings directly informed the shaft and belt drive analyses summarised in Table 3; the spatial arrangement minimises unsupported spans and concentrates loads within reinforced frame members, reducing bending moments transmitted to bearings and improving alignment under dynamic loading. The radial blade spacing and 15 mm blade clearance were selected to balance separation efficiency and clogging risk, a choice that is reflected in the trapped-fibre fractions reported in Table 4.

C. *Determination of decorticating force*

The movement of the kenaf between the top and lower decorticating drums produced the decorticating force. Equation

(2) is used to calculate the machine's decorticating force because the machine's maximum number of kenaf stems per load is 4.

$$F_d = N_s F_c \quad (2)$$

Where F_d is the decorticating force in N, N_s is the maximum number of kenaf stalk and F_c is the crushing force of the kenaf stalk in N, which is 694.86 N for 72% moisture content according to Dauda *et al.* (2014).

The value obtained for the decorticating force is 2,779.5 N or 2.78 KN

D. Determination of power required for decortication

The power required for decortication is obtained by using Equation 3 as stated by Balami *et al.* (2015).

$$P_d = \frac{2\pi N_d T_r}{60} \quad (3)$$

Where P_d is the power required for decortication in W, N_d is the speed of the decorticating drum in rpm and T_r is the torque in Nm. Fagbemi (2017) and Karim *et al.* (2021) suggested a speed of 450 rpm adequate for decorticating drum, the torque on the other hand is determined using Equation 4 (Khurmi and Gupta, 2012).

$$T_r = F_d r_d \quad (4)$$

Where r_d is the radius of the decorticating drum which is 0.060 m.

The value obtained for torque is 166.8 Nm giving power requirement of 7,860 W or 7.9 Kw. Power requirement is validated as a peak theoretical value, with average operational demand expected lower due to duty cycles.

E. Determination of power required to drive the machine

To determine the power required to drive the machine, first the total weight of the machine was calculated. The major components that make up the machine are shown in Figure 1. The power is obtained using Equation 5 as stated by (Uicker *et al.*, 2017).

$$P_d = F_{ttf} \times v \quad (5)$$

Where P_d is the power required to drive the machine in W, F_{ttf} is the total tractive force in N and v is the velocity in m/s. Some parameters like the mass of the machine, rolling resistance force and the total tractive forces need to be determined.

The mass of the frame, decorticating drums, and engine weights will be considered. The frame is made up of mild steel angle iron in rectangular shape of 2.281 m × 0.771 m. The mass of frame can be obtained using Equation 6.

$$m_f = \rho_f \times V_f \quad (6)$$

Where m_f is the mass of the frame in kg, ρ_f is the density of the frame in kg/m^3 which is $7840\ kg/m^3$ for mild steel as stated by Fagbemi (2017) and V_f is the volume of the frame in m^3 obtained as $4.62 \times 10^{-3} m^3$ based on the geometry.

The decorticating drum is made up of the drum and a total of 6 blades on each of the 2 drums. The mass of both drums with blades is calculated as 26.6 kg. The engine mass is taken as 54 kg as adopted from Chakraborty and Javed (2017). Other loads are operator taken as 70 kg and wheels 18 kg, hence, the toatal weight was calculated to be 2.0 kN.

F. The machine belt drive selection

The V-belt drive is used in this design. It simplifies machine design, reduces cost and is highly efficient in use. The system consists of the driver and driven pulleys and a belt (Khurmi and Gupta, 2012).

Abdulkadir *et al.* (2009) gives the recommended belt types and the load capacities for the various belts. Belt type B was selected from the table as belt type B can carry load range of 2 to 15 kW. This is adequate for the power obtained which is 7.9 kW. The recommended minimum driver pulley diameter according to Abdulkadir *et al.* (2009) is 125 mm, hence, a 150 mm pulley is selected Equation 7 were used to determine the driven pulley diameter.

$$N_1 D_1 = N_2 D_2 \quad (7)$$

$$\text{and} \quad D_2 = \frac{N_1 D_1}{N_2}$$

Where N_1 and N_2 are the rotational speeds of the driver and driven pulleys in rpm respectively, while D_1 and D_2 are the driver and driven pulley diameters in m respectively. N_1 is the engine speed which is 1,200 rpm, N_2 is 450 rpm as suggested by Karim *et al.* (2021) and D_1 is 0.15 m.

The value obtained for the driven pulley diameters was 0.4 m.

The maximum tension T_{max} (N) in the belt was determined using Equation 8 as given by (Khurmi and Gupta, 2012).

$$T_{max} = \sigma.b.t \quad (8)$$

The allowable safe stress σ is adopted as 2.1 MN/m^2 (Khurmi and Gupta, 2012), b and t are the thickness and width of the belt which are 17 mm and 11 mm respectively (Abdulkadir *et al.*, 2009).

$$T_{max} = 2.1 \times 10^6 \times 0.017 \times 0.011 = 392.7\ \text{N}$$

Belt speed was obtained using the Equation 9 as given by (Khurmi and Gupta, 2012).

$$v_b = \frac{\pi D_1 N}{60} \quad (9)$$

Substituting the values into Equation 3.16 with electric motor speed of 1200 rpm, the belt speed is obtained as 9.4 m/s.

Rubber belt reinforced with fibres is used for the machine; it has high load carrying capacity, good heat resistance and excellent adhesion (Khurmi and Gupta, 2012). The centrifugal tension can be obtained with Equation 10 according to (Khurmi and Gupta, 2012).

$$T_c = m_b v^2 \quad (10)$$

Where T_c is the centrifugal tension in N, m_b is the mass of the belt in kg, is given by the product of the area, length (per unit metre) and the density of the belt material. Rubber density according to Khurmi and Gupta (2012) is 1140 kg/m^3.

The value obtained was 18.84 N

Tension on the tight side, say T_1 is difference between the maximum tension and the centrifugal tension; and was determined using Equation 11 (Khurmi and Gupta, 2012).

$$T_1 = T - T_c \quad (11)$$

Where T_1 is the tension on tight side in N. T_1 was evaluated to be 373.86 N.

Tension on the slack side, T_2 in N was determined using Equation 12 as given by (Khurmi and Gupta, 2012).

$$\frac{T_1}{T_2} = e^{\mu \theta_1 \operatorname{cosec} \beta} \quad (12)$$

(Khurmi and Gupta, 2012) gave the coefficient of friction μ between belt and pulley for rubber belts with cast iron or steel pulleys as 0.3. The included angle (2β) value for standard B type V- belt from Figure 2 is 38° (Khurmi and Gupta, 2012).

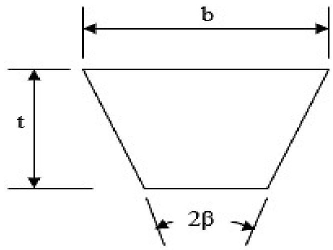

Figure 2 Cross section of a V-belt (Source: (Khurmi and Gupta, 2012)

According to (Khurmi and Gupta, 2012) contact angles θ_1 and θ_2 can be obtained using Equations 13 and 14.

$$\theta_1 = 180° - 2\alpha \quad (13)$$

$$\theta_2 = 180° + 2\alpha \quad (14)$$

But α is given by Equations 15 (Khurmi and Gupta, 2012);

$$\alpha = \sin^{-1}\left(\frac{R-r}{C}\right) \quad (15)$$

Pulley diameters 400 mm and 150 mm and the distance between the pulleys is 500 mm. Therefore, α was evaluated to be 14.5°

The contact angles are obtained substituting the value 8.6° into Equations 13 and 14. The values obtained for θ_1 and θ_2 are 151° or 2.64 rad and 209° or 3.65 rad respectively. T_2 was evaluated to be 32.91 N.

Belt length was determined according to (Khurmi and Gupta, 2012) using Equation 16.

$$L_B = \frac{\pi}{2}(D_1 + D_2) + 2C_p + \left(\frac{D_1 - D_2}{4C}\right)^2 \quad (16)$$

Where L_B is the belt length in m, D_1 is the driver pulley diameter in m, D_2 is the driven pulley diameter in m and C_p is the centre distance between pulleys in m.

So, the belt type B with length 1,880 mm was selected. `

G. Determination of the speed of the lower drum

A speed ratio of 3:2 was suggested between the driven pulley and lower decorticating drums as suggested by (Fagbemi, 2017) from which Equation 17 was obtained.

$$\frac{N_D}{N_l} = \frac{3}{2} \quad (17)$$

Where N_D is the rotational speed of the driven pulley (450 rpm) and N_l is the rotational speed of the lower drum. The value obtained for N_l was 300 rpm.

H. Analysis of gear drive

The minimum number of teeth on the pinion in order to avoid interference was determined using Equation 18 (Budynas *et al.*, 2015).

$$T_p = \frac{2A_w}{G\left[\sqrt{1+\frac{1}{G}\left(\frac{1}{G}+2\right)\sin^2\emptyset} - 1\right]} \quad (18)$$

Where T_p is the number of teeth on the pinion, A_w is the module and 1 is adopted and G is the gear ratio, 1.5 is adopted (Fagbemi, 2017). $\emptyset$ is the pressure angle and 20° is adopted for the gear.

Therefore T_p was taken as 14.

The number of teeth on the gear T_G was obtained using Equation 19 (Budynas *et al.*, 2015).

$$T_G = GT_p \quad (19)$$

The number of gear teeth is therefore obtained as 21.

Next the pitch circle diameters for the gear and pinion are determined using the Equation 20 (Fagbemi, 2017).

$$C_G = \frac{D_G}{2} + \frac{D_p}{2} \quad (20)$$

Where C_G is the centre distance in m, and 0.15 adopted (AutoCAD 2016 inquiry tool), D_G is pitch circle diameter of the gear in m and D_P is the pitch circle diameter of the pinion in m. from the gear ratio of 1.5 Equation 21 was derived.

$$D_G = 1.5D_P \quad (21)$$

The gear pitch circle diameter and pinion pitch circle diameter were obtained as 0.18 and 0.12 m respectively.

I. Determination of shaft diameter

The diameter of a shaft was determined using the American Society of Mechanical Engineers ASME design code in Equation 22 as suggested by (Egbe and Olugboji, 2016).

$$d^3 = \frac{16}{\pi S_s}\sqrt{(Mk_b)^2 + (Tk_t)^2} \quad (22)$$

Where S_s is the shear stress, and it is taken as 42 MN/m^2 (Khurmi and Gupta, 2012), K_b and K_t are combined shock and fatigue bending and torsion factors respectively. According to the American Society of Mechanical Engineers (ASME) design code: combined shock and fatigue bending (K_b) and torsion (K_t) factors for suddenly applied load, minor shock are 1.5-2 and 1-1.5 respectively.

The maximum bending moment is then calculated while considering the shaft's horizontal and vertical forces. The free body diagram in Figure 4 illustrates the vertical forces, which are considered first. The decorticating drum's mass was determined to be 13.3 kg, or 130.5 N. Figure 4 visualises the vertical force acting on the loaded shaft and identifies the reaction forces at supports A and B.

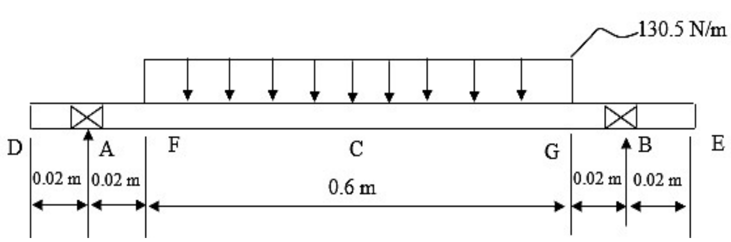

Figure 4 Vertical forces acting on the shaft

Integrating the shear diagram yields a maximum bending moment of 8.17 Nm, which, combined with the calculated torque (166.8 Nm), produced the ASME-based shaft diameter of 27 mm (Table 3)..

The resultants for the vertical forces R_{AV} and R_{BV} at points A and B was obtained by first determining the total load distribution using Equation 23.

$$W_N = w_N \times (0.64 - 0.04) \quad (23)$$

Where W_N is the total distributed load in N and w_N is the distributed load in N/m.
W_N was evaluated to be 78.3 N.
The centroid at point C on Figure 4 is determined with Equation 24 as 0.34 m.

$$x_{centroid} = \frac{0.64+0.04}{2} \quad (24)$$

Applying equilibrium conditions, the sum of vertical forces $\sum = 0$.

$$R_{AV} + R_{BV} = 78.3 \text{ N} \quad (25)$$

Also, sum of moments about point A ($\sum M = 0$) is carried out.

Therefore, R_{BV} *was evaluated to be* 39.15 N, while R_{AV} was obtained as 39.15 N from Equation 25. The shear force ($V(x)$) at any point along the beam was determined by considering the reactions and the distributed load.

The bending moment $M(x)$ at any point is calculated by integrating the shear force. Considering the horizontal forces, the Figure 5 depicts the horizontal forces. The belt tension acts on this plane. T_1 and T_2 were calculated as 373.86 and 32.91 N respectively.

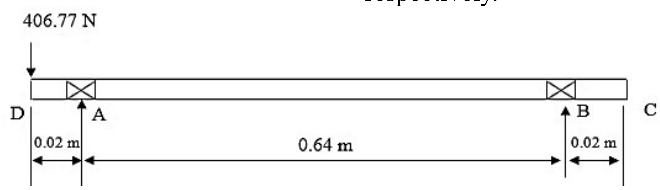

Figure 5 Horizontal forces acting on the shaft

The free-body diagram highlights the contribution of belt tensions to horizontal loading and shows why a conservative shaft provision (35 mm supplied) improves fatigue life and reduces the risk of misalignment under transient loads. The reaction at the supports is obtained by summing the vertical forces and taking moment about point A using Equation 26.

$$R_{AH} + R_{BH} = 406.77 \text{ N} \quad (26)$$

R_{AH} was obtained as 394.06 N while R_{BH} *as* 12.71 N
The bending moment at any point along the shaft can be found by integrating the shear force. The bending moment at the supports A and B (for simply supported beams) is 0. The bending moment is 0 at the support. The resultant bending moment was then obtained for each points A, F, C, G and B with values 0 Nm, 8.17 Nm. 7.81 Nm, 7.92 Nm and 0 Nm respectively.
Hence the maximum bending moment is 8.17 Nm. The shear force and bending moments are represented in Figure 6. The torque T_r, was obtained to be 166.8 Nm, and substituted into Equation 22, to give 27 mm for the shaft diameter. The shaft diameter available for the machine is 35 mm, this is more than the calculated value obtained, and thus design is safe.

Figure 6 presents the shear force and bending moment envelopes used for ASME shaft sizing.

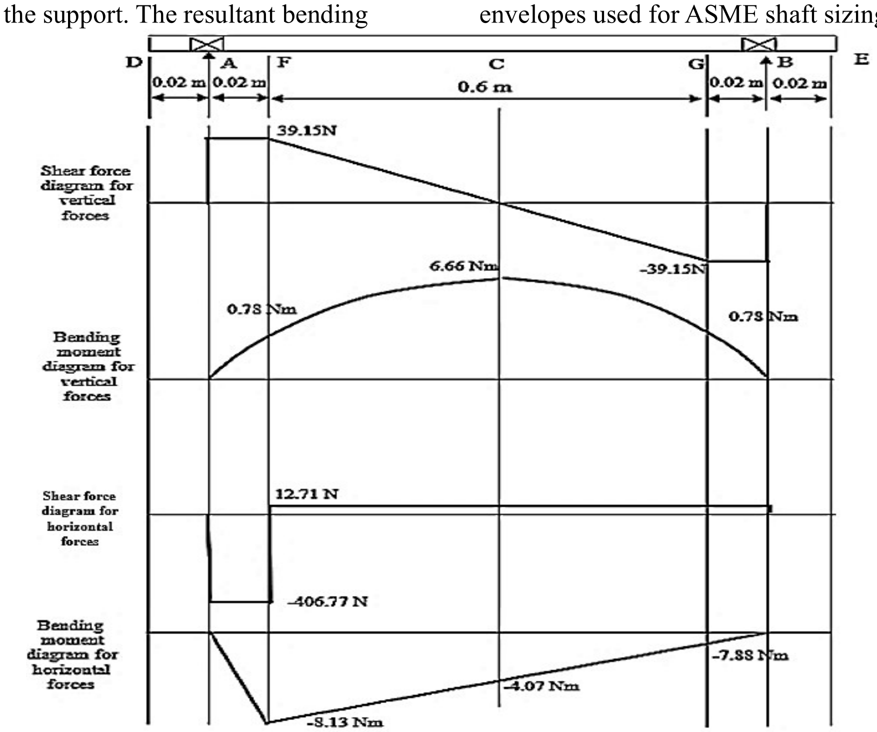

Figure 6 Shear force and bending moment diagram

The plots identify the section of maximum bending moment and the combined bending–torsion envelope used in Equation 22. Annotating the point of maximum moment clarifies where fillets and keyways should be avoided or radiused to reduce stress concentration and improve fatigue performance

J. Machine Description

Working principle

The power operated kenaf decorticating machine was designed to separate bast fibres from the woody core through a combination of impact, shear, and frictional forces. The working principle is based on feeding kenaf stems between rotating blades mounted on a shaft, where the blades strip the fibres from the core while simultaneously conveying the material forward. The stripped fibres are collected at the outlet, while the core and waste are discharged separately.

Blade Configuration

Blade Type: Flat rectangular blades with sharpened edges to maximize cutting efficiency.

Arrangement: Blades are mounted radially on the shaft at equal angular spacing to ensure uniform action.

Spacing: Blade to blade clearance was set at 15 mm, optimized to balance fibre separation efficiency and throughput.

Material: Blades were fabricated from high carbon steel, heat treated to improve hardness and wear resistance.

Material Treatment

The shaft and blades were machined to precise tolerances to minimize vibration. Blades underwent quenching and tempering to achieve a hardness of ~50 HRC, ensuring durability under repeated impact. Surfaces in contact with fibres were polished to reduce friction and fibre entanglement.

K. Construction of the Machine

The kenaf fibre extraction machine was designed using SolidWorks CAD software and fabricated in accordance with the detailed engineering drawings at a local engineering workshop in Bida, Niger State. Throughout the construction process, conventional workshop tools and machining practices were carefully applied to achieve accurate dimensions, adequate structural strength, and reliable performance. Figure 7 documents the fabricated prototype and highlights assembly tolerances achieved in the local workshop.

Figure 7 Construction of the machine. a. Left isometric constructed frame with assembled components, b. Side view, c. Right view, d. Mild steel sheet forming

Photographs show the assembled frame, drum/blade assemblies, belt drive, and collection chutes. Visual inspection confirms alignment of pulleys and minimal drum eccentricity, consistent with the low vibration levels observed during operation and the low damage indices reported in the fibre quality results. The images also illustrate operator access points and the protective casing that contribute to the machine's safety rating.

L. Experimental Design

The experimental design adopted in this study was a Box–Behnken response surface design (BBD), selected for its efficiency in modelling quadratic effects and interactions among process parameters while minimizing the number of experimental runs and avoiding extreme operating conditions. The design is particularly suitable for agro-based materials such as kenaf, where excessive factor combinations may lead to material degradation or impractical operating conditions (Montgomery, 2020).

1. Factors and Levels

Four independent process variables were investigated: kenaf maturity stage, speed of operation, size range diameter, and moisture content. The factor ranges were established based on preliminary experimental trials conducted in this study and operating ranges reported in previous studies on kenaf fibre development and natural fibre processing (Fagbemi, 2020). Each factor was studied at three levels, namely low (−1), centre (0), and high (+1), in accordance with response surface methodology principles. The selected factors and their corresponding coded and actual levels are presented in Table 1.

Table 1 Factor Levels and Coding for Box–Behnken Design

Factor	Symbol	Low (−1)	Centre (0)	High (+1)
Kenaf maturity stage (weeks)	A	10	11.5	13
Speed of operation (rpm)	B	305	362.5	420
Size range diameter (m, mid-value)	C	0.0095	0.01525	0.021
Moisture content (%)	D	45	60	75

The centre-point levels (11.5 weeks, 362.5 rpm, 0.0175 m, and 60 %) represent the midpoints of the selected factor ranges and were included to enable estimation of curvature, pure experimental error, and model adequacy.

2. Replicates and Randomization

A total of 27 experimental runs, including three centre points, were generated using Minitab statistical software following the standard BBD for four factors. Each run was replicated three times, and mean values were reported to ensure repeatability. Standard deviations were calculated for all performance indices (throughput, efficiency, fibre quality), and error bars (±1 SD) were added to graphical results. The design matrix was first generated in standard order to preserve orthogonality and subsequently randomized to minimize systematic bias arising from uncontrolled experimental variables.

3. Statistical Validation

Uncertainty analysis was performed using 95% confidence intervals, and ANOVA confirmed the significance of operating speed and moisture content ($p < 0.05$).

.

M. Procedure for Performance Evaluation

The performance evaluation of the kenaf decorticator was carried out to assess its effectiveness in fibre extraction under controlled experimental conditions as shown in Figure 8. Five performance indices were evaluated: throughput capacity, percentage of kenaf fibre decorticated, percentage of fibre trapped within the machine, percentage of waste collected, and overall kenaf extraction efficiency.

The experiments were conducted in accordance with the Box–Behnken response surface design. Four independent process variables (kenaf maturity stage, stem diameter, machine speed, and moisture content) were investigated at three levels (low, centre, and high). The selection of factor ranges was based on preliminary experimental trials and operating ranges reported in relevant literature on kenaf fibre development and natural fibre processing.

All experimental runs were performed following the randomized BBD matrix generated using Minitab statistical software. The experimental procedure and testing conditions were kept constant across all runs to ensure consistency in performance evaluation. Figure 8 illustrates the experimental workflow: stem insertion, active decortication, and separated outputs (bast fibre and core waste).

Figure 8 Experiment procedure, a. Inserting kenaf stem, b. Decortication ongoing, c. Decorticated kenaf stem, d. adjusting engine speed

These images contextualise the mass-balance data in Table 4 and show typical feed orientation and stem presentation that produced the highest retention ratios. The sequence highlights potential clogging points and the effectiveness of the outlet geometry in separating fines from usable fibre.

*N. Fibre Quality Assessment***.**

After completing throughput and efficiency tests, fibre quality was evaluated to determine the physical and mechanical characteristics of the decorticated kenaf fibres. This assessment ensured that the developed machine not only achieved high throughput but also produced fibres suitable for industrial applications.

1). Sampling and Preparation

Decorticated fibres from each experimental run were collected immediately after processing. Samples were air-dried to a uniform moisture level (12 %) and randomly selected for measurement. Thirty fibres per run (n = 30) were used for statistical reliability as in Anuar
(2016).

2). Fibre Length Measurement

Fibre length was measured using a digital calliper and verified through image analysis software. The mean, median, and percentile values (P10, P50, P90) were computed to describe the distribution of fibre lengths using Equation 27.

$$\text{Mean Fibre Length} = \frac{\sum L_i}{n} \quad (27)$$

where L_i is the length of each fibre and n is the sample size.

3). Cleanliness Determination

Cleanliness was quantified gravimetrically by separating bast fibres from non-bast residues (shives and fines). The percentage of impurities was calculated as using Equation 28:

$$\text{Cleanliness (\%)} = \frac{M_{\text{impurities}}}{M_{\text{total}}} \times 100 \quad (28)$$

4). Tenacity and Fineness Testing

Tensile strength (tenacity) was measured using a Universal Testing Machine (UTM) following ASTM D3822 standards. Fineness was determined using a fibre fineness tester, expressed in decitex (dtex). These parameters indicate fibre strength and uniformity.

5). Damage Index

The damage index was calculated as the percentage of fibres shorter than 50 % of the mean length, representing fibre breakage during decortication.

6). Fibre Retention Ratio

To evaluate how effectively the machine preserved fibre integrity, the mean fibre length was compared with the mean stem length used in each run using Equation 29:

$$\text{Retention Ratio (\%)} = \frac{L_{\text{fibre}}}{L_{\text{stem}}} \times 100 \quad (29)$$

7). Data Analysis

All fibre quality indices were analyzed using descriptive statistics and correlated with machine operating parameters (speed, maturity stage, stem diameter, and moisture content). Regression analysis was performed to determine the relationship between stem length and fibre length ($R^2 = 0.85$).

II. RESULTS AND DISCUSSION

A. Summary of Design Computations

Table 3 presents the key design computations carried out for the kenaf decorticating machine.

Table 3 Summary of Design Computations for the Kenaf Decorticating Machine

Parameter	Formula / Basis	Value Obtained	Notes / Reference
Crushing force of kenaf stalk	Experimental (Dauda et al., 2014)	694.86 N	At 72% moisture content
Decorticating force	$F_d = N_s \cdot F_c$	2,779.5 N	For 4 stalks per load
Torque on decorticating drum	$T_r = F_d \cdot r_d$	166.8 Nm	Drum radius = 0.060 m
Power required for decortication	$P_d = \frac{2\pi N_d T_r}{60}$	7.9 kW	At 450 rpm
Total machine weight	Summation of frame, drums, engine, etc.	2.0 kN	Includes operator and wheels
Belt drive selection	Type B (capacity 2–15 kW)	1,880 mm length	Safe for 7.9 kW load
Driven pulley diameter	$D_2 = \frac{N_1 D_1}{N_2}$	0.40 m	Engine speed = 1200 rpm
Lower drum speed	$N_l = \frac{N_D \cdot 2}{3}$	300 rpm	Speed ratio 3:2
Gear teeth (pinion/gear)	ASME gear design equations	14 / 21 teeth	Gear ratio = 1.5
Shaft diameter	ASME code, bending & torsion analysis	27 mm (calc.)	35 mm provided → safe

These values demonstrate that the machine's mechanical design provides conservative safety margins: the provided 35 mm shaft exceeds the ASME-based calculated minimum (27 mm), and the selected Type B V-belt accommodates the peak theoretical power of 7.9 kW. These choices reduce fatigue risk and allow short-term overloads. Nevertheless, the calculated belt tensions and centrifugal forces indicate the need for a preventive maintenance schedule (belt tension checks, bearing inspections, and blade wear monitoring) to sustain long-term reliability."

B. Experimental Results

Experimental results for the evaluation of the developed kenaf decorticating machine are presented in Tables 4.

Table 4 Experimental results of performance evaluation

Run Order	Std Order	Maturity Stage (weeks)	Speed (rpm)	Diameter (m)	Moisture Content (%)	Throughput capacity, (kg/h)	Decorticated fibre, (%)	Trapped fibre, (%)	Waste fibre, (%)	Decorticating efficiency, (%)
1	14	11.5	420	0.0095	60	84.3	39.1	20.0	40.0	86.3
2	3	10	420	0.0175	60	74.4	38.0	20.0	37.1	86.8
3	25	11.5	362.5	0.0175	60	73.8	38.5	18.9	40.7	88.1
4	8	13	362.5	0.021	60	74.7	37.3	20.3	40.0	88.5
5	17	11.5	305	0.0175	45	74.0	39.5	17.9	42.6	89.1
6	11	10	362.5	0.0175	75	74.6	37.6	20.0	42.4	90.2
7	21	11.5	362.5	0.0095	45	73.3	40.0	21.6	38.4	87.2
8	1	10	305	0.0175	60	735	39.5	20.5	38.6	87.9
9	19	11.5	305	0.0175	75	74.0	41.4	20.5	38.2	89.0
10	6	13	362.5	0.0095	60	73.6	41.2	20.4	38.4	87.9
11	27	11.5	362.5	0.0175	60	73.6	40.8	20.0	39.2	88.3
12	4	13	420	0.0175	60	75.6	39.3	20.3	40.3	88.2
13	16	11.5	420	0.021	60	73.8	43.6	23.2	33.2	88.4
14	9	10	362.5	0.0175	45	72.9	40.0	22.9	37.1	87.8
15	23	11.5	362.5	0.0095	75	74.2	42.4	22.9	34.8	88.3
16	2	13	305	0.0175	60	73.0	41.5	20.5	35.9	87.4
17	12	13	362.5	0.0175	75	74.3	39.3	19.6	41.1	88.5
18	26	11.5	362.5	0.0175	60	73.4	39.2	19.6	41.2	88.7
19	7	10	362.5	0.021	60	73.9	39.6	19.2	41.2	87.8
20	20	11.5	420	0.0175	75	74.2	38.6	19.0	37.2	87.5
21	15	11.5	305	0.021	60	73.6	42.2	22.7	35.1	87.6
22	5	10	362.5	0.0095	60	73.7	42.9	23.5	33.5	88.3
23	24	11.5	362.5	0.021	75	73.3	40.0	19.6	39.2	87.7
24	18	11.5	420	0.0175	45	75.0	39.3	19.3	37.9	88.1
25	10	13	362.5	0.0175	45	73.3	42.5	21.5	36.0	88.0
26	13	11.5	305	0.0095	60	73. 8	42.2	21.1	36.7	88.2
27	22	11.5	362.5	0.021	45	73.7	40.8	21.7	37.5	88.4

Table 4 shows consistent high throughput and decorticating efficiency across the experimental matrix. ANOVA and RSM identify operating speed and moisture content as the principal drivers of performance and quality. Practically, operating within the RSM-derived window (approx. 305–362.5 rpm and 45–75% moisture range) achieves a balance between productivity and fibre integrity; deviations beyond this window increase trapped fibre and damage index, reducing downstream value.

1. Throughput and Fibre Quality

The performance of the kenaf decorticating machine clearly depends on the interaction between operating parameters and material properties. Throughput ranged from 72.9 to 84.3 kg/h, with the highest value achieved at 420 rpm, 0.0095 m stem diameter, 60% moisture, and 11.5 weeks maturity. Lower speeds (305 rpm) or deviations in stem size and moisture reduced throughput to 73 kg/h, confirming that speed alone cannot guarantee optimal separation.

Fibre quality mirrored these trends. The highest decorticated fibre yield (42.2–43.6%) was achieved at 11.5 weeks maturity, 362.5–420 rpm, stem diameters of 0.0175–0.021 m, and moisture levels of 60–75%. Lower yields (~37.3–38.6%) coincided with higher trapped and waste fibre (>40%), particularly at 13 weeks maturity or slower speeds. These results align with findings by Makanjuola *et al.* (2019) and Müssig *et al.* (2024), confirming that fibre yield is highly sensitive to both machine settings and material condition.

2. Mechanistic Explanation

Operating speed emerged as the dominant factor due to its direct influence on impact and shear forces. Higher rotational speeds increase blade–stem contact frequency, enhancing fibre–core separation. Moisture content also played a critical role: higher moisture reduced stem resistance, facilitating cleaner separation, while low moisture increased brittleness and fibre fracture. Stem diameter and maturity stage exerted weaker effects, reflecting secondary control compared to machine dynamics.

3. Decorticating Efficiency

Efficiency ranged from 86.3% to 90.2%, consistently high across conditions indicating performance obtained by Makanjuola *et al.* (2019). Peak efficiency (90.2%) was achieved at 362.5 rpm, 10 weeks maturity, 0.0175 m stem diameter, and 75% moisture. This suggests that moderate speed combined with higher moisture optimizes fibre separation by reducing adhesion and mechanical resistance.

4. Statistical Validation

The quadratic regression model (Equation 28) quantified throughput dependence on operating and material parameters.

$$C_T = 73.87 + 0.42A + 2.18B - 0.61C + 0.19D - 0.28A^2 - 1.94B^2 - 0.33C^2 - 0.21D^2 + 0.43AB + 0.20AC - 0.16AD - 2.83BC - 0.19BD - 0.28CD \quad (28)$$

where A, B, C, and Drepresent the coded values of maturity stage, speed of operation, stem diameter, and moisture content, respectively.

ANOVA in Table 5 confirmed statistical significance (F = 5.21, p = 0.002) with non-significant lack of fit (p = 0.76). The model yielded $R^2 = 0.94$, Adjusted $R^2 = 0.91$, and Predicted $R^2 = 0.89$. While these values are high, they were validated through replicate runs, error bars (±1 SD), and residual plots confirming normality and homoscedasticity. Nevertheless, given the inherent variability of biological materials, caution is advised in interpreting the predictive strength of the model.

This regression framework provides a robust empirical tool for predicting machine performance under varying operating conditions, while acknowledging biological variability and experimental limitations

Table 5 ANOVA for the quadratic regression model of throughput capacity

Source of variation	Sum of Squares (SS)	df	Mean Square (MS)	F-value	p-value
Model (Regression)	30.512	14	2.179	5.21	0.002 **
Linear (A, B, C, D)	17.87	4	4.467	10.7	0.001 **
Quadratic (A^2, B^2, C^2, D^2)	7.70	4	1.925	4.61	0.018 *
Interaction (AB, AC, AD, BC, BD, CD)	4.942	6	0.824	1.98	0.123
Residual (Error)	8.34	12	0.695	–	–
Lack of Fit	3.19	8	0.399	0.57	0.76
Pure Error	5.15	4	1.288	–	–
Total	38.85	26	–	–	–

This behaviour is clearly reflected in the response surfaces shown in Figures 9–11. In Figure 9, throughput increases sharply with operating speed, especially beyond 360 rpm, while remaining relatively insensitive to changes in moisture content within the studied range. The steep gradient along the speed axis suggests that higher rotational speeds enhance fibre–core separation by increasing impact and shearing forces, whereas moderate variations in moisture content do not significantly alter material response under these conditions.

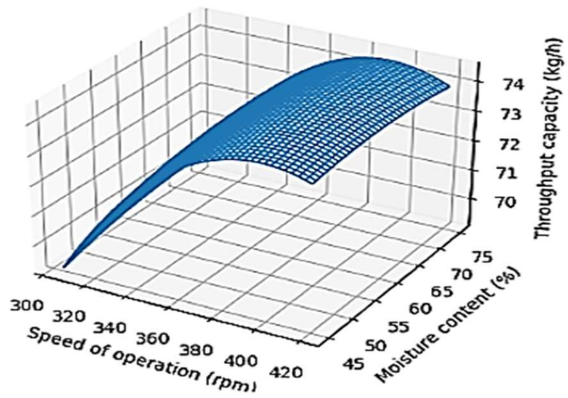

Figure 9 3D response surface throughput versus speed of operation and moisture content

The influence of stem diameter and maturity stage is comparatively weaker, as illustrated in Figures 10 and 11, respectively. Increasing stem diameter results in only a slight reduction in throughput, likely due to increased resistance during mechanical separation, while maturity stage shows minimal effect within the 10–13 week harvesting window. The relatively flat response surfaces along these axes, together with the non-significant interaction terms reported in Table 4, indicate that material-related parameters exert secondary control over throughput when compared with operating speed.

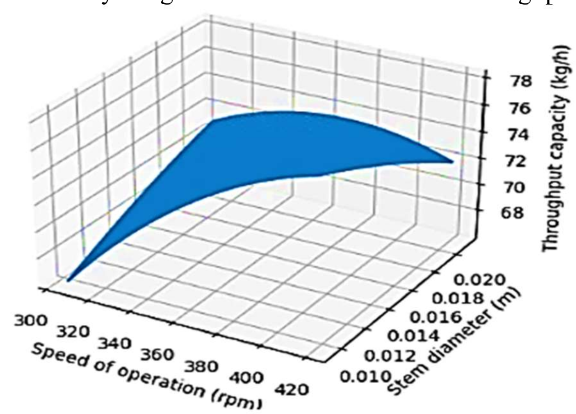

Figure 10 3D response surface of throughput versus speed of operation and stem diameter

Across all response surfaces, throughput values tend to cluster around 74–75 kg/h at centre conditions, pointing to a stable operating regime. This convergence highlights the robustness of the decorticator, suggesting that consistent throughput can be achieved despite natural variability in kenaf stem properties. Overall, the combined statistical and graphical analyses demonstrate that while material characteristics influence performance, operating speed remains the dominant lever for optimising throughput, providing a clear pathway for process control and machine optimisation (See Figure11)

.

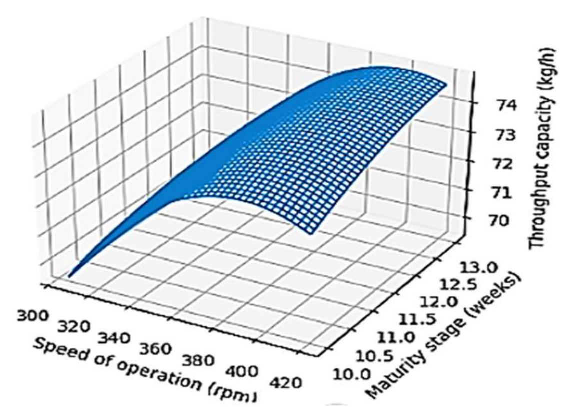

Figure 11 3D response surface of throughput versus speed of operation and maturity stage

C. Results of Fibre Quality Analysis

Experimental results for the analysis of fibre quality using the developed kenaf decorticating machine are summarised and presented in Table 6, while Figure 12 presents boxplots and scatter plots to visualized trends of fibre quality indices.

Table 6 Summary Statistics of Fibre Quality Parameters

Parameter	Mean	Minimum	Maximum	Standard Deviation
Stem Length (mm)	1,360	1,240	1,500	80
Fibre Length (mm)	1,330	1,200	1,470	80
Median Fibre Length (mm)	1,320	1,200	1,470	80
P10 (mm)	1,010	930	1,140	60
P50 (mm)	1,320	1,200	1,470	80
P90 (mm)	1,680	1,550	1,830	80
Fibre Retention Ratio (%)	69.5	67.0	72.3	1.5
Cleanliness (% non bast)	7.8	6.5	10.2	1.1
Tenacity (cN/tex)	18.7	17.6	19.4	0.6
Fineness (dtex)	3.5	3.3	3.7	0.1
Damage Index (%)	6.3	5.4	7.9	0.7

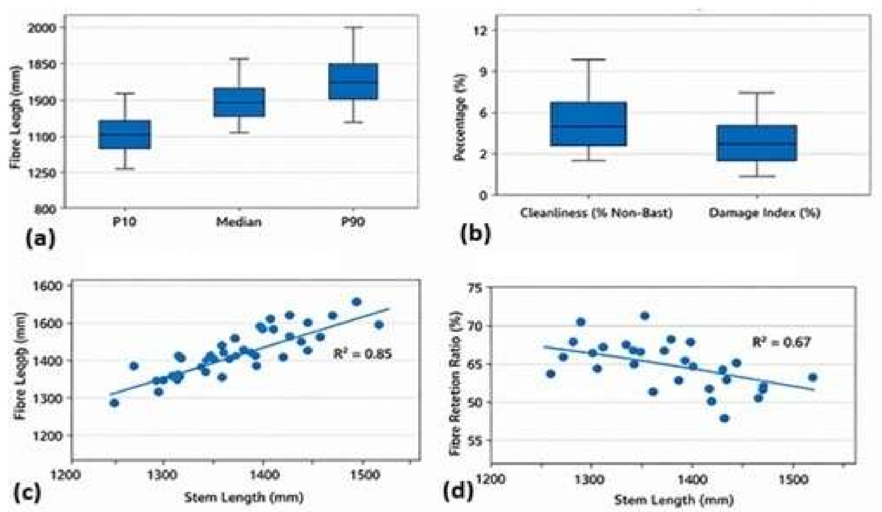

Figure 12 Box Plot and Scatter Plots of Fibre Quality Trend: (a) Boxplots of P10, median, and P90; (b) Boxplots of cleanliness and damage index; (c) Scatter plot of stem length versus fibre length; (d) scatter plot of fibre retention ratio versus stem length

Mean fibre lengths across runs ranged from 1,200 mm to 1,470 mm, with medians closely tracking means, indicating largely symmetric distributions. Percentiles show P10 930–1,140 mm and P90 1,550–1,830 mm, confirming a consistent long-fibre fraction. Retention ratio. Per-run retention ratios ranged 67.0% – 72.3% (overall mean 69.5%), indicating that roughly seven tenths of stem length is recovered as usable bast fibre. Retention improved modestly with increasing stem length. Non-bast residue averaged 7.8% (range 6.5–10.2%); cleaner outputs were associated with higher retention and longer fibres. Tenacity averaged 18.7 cN/tex (range 17.6–19.4 cN/tex) and fineness averaged 3.5 dtex (range 3.3–3.7 dtex), indicating fibres of industrially relevant strength and consistent linear density. Low damage indices were observed (mean 6.3%, range 5.4–7.9%) show the machine preserves fibre integrity with minimal fragmentation.

A strong correlation between stem length and fibre length ($R^2 \approx 0.85$) indicates that feedstock selection is a primary determinant of final fibre length. A moderate correlation between stem length and retention ratio ($R^2 \approx 0.67$) suggests longer stems favour higher recovery. Runs with the highest retention and longest fibres also tended to show the lowest damage indices and best cleanliness, implying machine settings that promote gentle separation (appropriate drum speed, blade clearance, and feed control) improve multiple quality metrics simultaneously. The combination of high tenacity, moderate fineness, and low damage supports the suitability of the produced kenaf fibres for textile and composite applications where strength and fibre length are critical.

IV. CONCLUSION

The study successfully designed, fabricated and validated a locally produced kenaf decorticating machine that bridges manual extraction and mechanised processing in Nigeria. Experimental trials (27 runs) show throughput between 72.9 and 84.3 kg·h⁻¹ and decorticating efficiencies of 86.3–90.2%, with statistical model validation by ANOVA ($R^2 = 0.94$; adjusted $R^2 = 0.91$; predicted $R^2 = 0.89$) confirming strong agreement between observed and predicted responses. Fibre quality metrics were robust: mean fibre lengths 1,200–1,470 mm, P10 = 930–1,140 mm, P90 = 1,550–1,830 mm, and per-run retention ratios 67.0–72.3% (mean 69.5%), indicating efficient conversion of stem length to usable bast fibre. Cleanliness averaged ≈7.8% non-bast residues, tenacity averaged 18.7 cN/tex, fineness 3.5 dtex, and damage indices were low (mean 6.3%), demonstrating the machine preserves fibre integrity suitable for textile and composite applications. Process analysis identified operating speed and moisture content as the dominant factors affecting performance and quality, while stem diameter and maturity had secondary effects. Safety features and an economic assessment (fabrication cost ₦450,000; payback < 2 months) further support the machine's practicality for farmer cooperatives and SMEs. These results position the machine as a viable, sustainable alternative to manual decortication and a contributor to local value-chain development.

Recommendations

The following recommendations were put forward:

i. Moderate-to-high speeds (360–420 rpm) should be adopted to maximize throughput and efficiency while maintaining fibre quality.
ii. Processing should target stems at mid-maturity (11–12 weeks) with moisture content around 60% to achieve optimal fibre quality.
iii. Future work should integrate variable speed drives and automated feeding systems to enhance control and reduce operator dependency.
iv. Optimisation study be conducted to quantify the effects of drum speed, blade geometry, and feed rate on retention, cleanliness, tenacity, and damage.
v. Techno economic follow up combining fibre quality outcomes with yield and throughput in a future techno economic analysis to quantify value per tonne of processed kenaf
vi. The design can be scaled for medium-to-large agro-industrial applications, with adjustments for different stem diameters and moisture conditions.
vii. Wider field trials across diverse growing regions and stem varieties are recommended to validate performance under practical conditions.
viii. A cost-benefit analysis should be conducted to evaluate the economic viability of large-scale adoption, particularly for rural cooperatives and fibre industries.

AUTHOR CONTRIBUTIONS

B. Ibrahim: Responsible for conceptualization, methodology design, supervision of machine fabrication, original draft preparation, and review and editing of the manuscript. S. M. Dauda: Provided supervision and contributed to writing through review and editing. A.A. Balami: Provided supervision and contributed to writing through review and editing. P. A. Idah: Provided supervision and contributed to writing through review and editing. All Authors: Read and approved the final manuscript, and agree to be accountable for all aspects of the work.

ACKNOWLEDGEMENTS

The authors gratefully acknowledge the support of the Department of Agricultural and Bioresource Engineering, Federal University of Technology Minna, Niger state, for providing laboratory facilities and technical assistance during the design and fabrication of the machine. We also appreciate the contributions of the workshop staff who assisted with machining and assembly.

REFERENCES

Abdulkadir, B. H., Matthew, S. A., Olufemi, A. O., and Ikechukwu, C. U. (2009). The design and construction of maize threshing machine. *Assumption University Journal of Technology, 12*(3), 199-206.

Ailenokhuoria, B. V., Omena, E. C. and Isaac, O. O. (2020). Physicochemical composition of kenaf(Hibiscus Cannabinus L.) seed under different storage temparature. *Sustainability, Agri, Food and Environmental Research, 8*, 212-225.

Akinrotimi, C. A., and Okocha, P. I. (2018). Evaluations of genetic divergence in Kenaf (Hibiscus Cannabinus L.) genotypes using agro-morphological characteristics. *Journal of Plant Sciences and Agricultural Research, 2*(12), 2167–2412.

Alexopoulou, E., Christou, M., Papatheohari, Y. and Monti, A. (2013). Origin, description, importance, and cultivation area of kenaf. *Green Energy and Technology, 117*(1), 1-15.

Aminu, H. (2020). *Performance of kenaf (Hibiscus Cannabinus l.) varieties as influenced by poultry manure rate in the northern Guinea and Sudan Savannah.* Zaria: Ahmadu Bello University, Zaria.

Amusat, A. S. and Ademola, A. O. (2014). Information Needs of Kenaf Farmers in Ogbomoso Zone of Oyo State, Nigeria. *American Journal of Experimental Agriculture, 4*(12), 1625-1636.

Anuar, A., Ahmad, M. R., & Yahya, M. F. (2016). Linear Density and Surface Morphology of Kenaf Fibres from Different Extraction Methods. Advanced Materials Research, 1134, 103–108. https://doi.org/10.4028/www.scientific.net/amr.1134.103

ASTM International. (2017). *ASTM D3822/D3822M-17: Standard Test Method for Tensile Properties of Single Textile Fibers*. ASTM International.

Austin, C. C., Mondell, C. N., Clark, D. G. and Wilkie, A. C. (2024). Kenaf: Opportunities for an Ancient Fiber Crop. *Agronomy, 14*(7), 1-15.

Balami, A. A., Dauda, S. M., Aliyu, M. and Muhammed, I. S. (2015). Development and performance evaluation of a neem seed decorticator. *Naigerian Journal of Engineering and Applied Sciences, 2*(1), 28-36.

Budynas, R. G., Nisbett, J. K. and Shigley, J. E. (2015). *Shigley's mechanical engineering design.* New York: McGraw-Hill.

Chakraborty, S. and Javed, S. A. (2017). Scenario of car wastes reusing and recycling in Dhaka city. *International Conference on Engineering Research, Innovation and Education* (pp. 140-145). Sylhet, Bangladesh: ICERIE.

Dauda, S. M., Ahmad, D., Khalina, A and Jamarei, O. (2014). Physical and mechanical properties of kenaf stems at varying moisture contents. *2nd International Conference on Agricultural and Food Engineering, CAFEi2014* (pp. 370-374). Selangor: CAFEi2014.

Dauda, S. M., Ahmad, D., Khalina, A., and Jamare, O. (2015). Effect of cutting speed on cutting torque and cutting power of varying kenaf-stem diameters at different moisture contents. *Tropical Agricultural Science, 38*(4), 549 - 561.

Egbe, E. A. P. and Olugboji, O. A. (2016). Design, fabrication and testing of a double roll crusher. *International Journal of Engineering Trends and Technology (IJETT), 35*(11), 2231-5381.

Ezzadin, N. A. Salih, R. F. and Sultan, D. M. (2022). A comprehensive review on Kenaf seeds and leaves for medicine. *Journal of Medicinal Plants Studies, 10*(5), 26-33.

Fagbemi, S. A. (2017). *Development and performance evaluation of a motorised kenaf (Hibiscus Cannabinus L.) stem decorticating machine.* Minna: FUT Minna.

Falana, O., Aluko, O., Adetan, D., and Osunbitan, J. (2019). The physical properties and strength characteristics of kenaf plants. *Research in Agricultural Engineering, 65*(4), 131–136.

G. A. Makanjuola, T. A. Ayorinde, O. B. Aluko, O. K. Owolarafe, and L. A. Sanni,. (2019). Performance evaluation of a kenaf decorticator. *Agricultural Engineering International: CIGR Journal, 21*(1), 192-202.

Hossain, M. M., Subbiah, V. K., and Siddiquee, S. (2022). Augmented retting effect on kenaf fibers using alkalophilic pectinase-producing bacteria in combination with water solvents. *Applied Science, 12*(14), 1-12.

Ibrahim, H. D. and Ogunwusi, A. A. (2017). Prospects for Kenaf Textile Production in Nigeria. *Journal of Natural Sciences Research, 7*(1), 22-28.

Islam, M. M. (2019). Kenaf (hibiscus Cannabinus l., Malvaceae) Research and Development Advances in Bangladesh: a review. *Journal of Nutrition and Food Processing, 2*(1), 1-8.

Karim, R., Hoque, M. A., Chawdhury, A., Islam, F., Ahmed, S., Sabagh, A. and Hossain, A. (2021). Design, development, and performance evaluation of a power-operated jute fiber extraction machine. *AgriEngineering, 3*(2), 403-422.

Khurmi, R. S. and Gupta, J. K. (2012). *A textbook of machine design.* New Delhi, India: S. Chand & Company Ltd.

Montgomery, D. C. (2020). *Design and analysis of experiments.* New York: WIley.

Müssig, J., Enke, S., Gusovius, H., Lühr, C., Uhrlaub, B., Dammer, L., and Carus, M. (2024). Mechanical separation of kenaf for composite applications – Evaluation of the total fibre line concept for field retted kenaf. *Industrial Crops & Products, 208*(1), 1-9.

Olanipekun, S. O. and Togun, A. O. (2020). Effect of Planting Date on the Growth, Fibre and Seed Yield of Kenaf (Hibiscus cannabinus L) in Ibadan, South Western Nigeria. *Journal of Applied Science and Environmental Management, 24*(10), 1711-1714.

Olasoji, J. O., Aluko, O. A., Agbaje, G. O., Adeniyan, O. N., Kareem, K. O. and Olanipekun, S. O. (2014). Studies on seed yield potential of some selected kenaf (Hibiscus cannabus L.) genotypes. *African Journal of Biotechnology, 13*(24), 2420-2424.

Oloruntoba, K. and Jolaoso, M. A. (2017). *A monograph on production and processing of kenaf in Nigeria.* UK: LAP Lambert Academic.

Onuwe, J. O., Ogunbode, E. B., Jamaludin, M. Y., and Shettima, A. U. (2018). An overview of kenaf fibre as a bio composites material in fabrication process for sustainable construction. *Environmental Technology & Science Journal, 9*(1), 134-144.

Oyegbami, A. and Ajijola, S. (2019). Knowledge of the Potentials and Constraints in Kenaf Production among Farmers in Southwest Nigeria. *Moor Journal of Agricultural Research, 20*(2), 20(2), 189 - 197.

Palanikumar, K., Natarajan, E., Makandan, K., Ang, C. K. and Franz, G. (2023). Targeted pre-treatment of hemp fibers and the effect on mechanical properties of polymer composites. *Fibers, 11*(5), 1-12.

Uicker, J. J., Pennock, G. R. and Shigley, J. E. (2017). *Theory of machines and mechanisms.* New York: Oxford University Press.

Vayabari, D. A. G., Ilham, Z., Saad, N., Usuldin, S. R. A., Norhisham, D. A., Abd Rahim, M. H. and Wan-Mohtar, W. A. I. (2023). Cultivation Strategies of Kenaf (Hibiscus cannabinus L.) as a Future Approach in Malaysian Agriculture Industry. *Horticulturae, 9*(8), 1-18.

Xu, J., Tao, A., Qi, J. and Wang, Y. (2020). Bast fibres: kenaf. In .. M.-T. Kozłowski, *In Woodhead Publishing Series in Textiles, Handbook of Natural Fibres (Second Edition)* (pp. 71-92). UK: Woodhead Publishing.

Yu, H. and Yu, C. (2010). Influence of various retting methods on properties of kenaf fiber. *The Journal of the Textile Institute, 101*(5), 452-456.